

Wave Properties of Isothermal Magneto-Rotational Fluids

M. Sharif *and Umber Sheikh

Department of Mathematics, University of the Punjab,
Quaid-e-Azam Campus Lahore-54590, Pakistan.

Abstract

In this paper, the isothermal plasma wave properties in the neighborhood of the pair production region for the Kerr black hole magnetosphere are discussed. We have considered the Fourier analyzed form of the perturbed general relativistic magnetohydrodynamical equations whose determinant leads to a dispersion relation. For the special scenario, the x -component of the complex wave vectors are numerically calculated. Respective components of the propagation vector, attenuation vector, phase and group velocities are shown in graphs. We have particularly investigated the existence of a Veselago medium and wave behavior (modes of waves dispersion).

Keywords: Black Hole Physics; GRMHD; Plasmas; Relativity; Waves; Equation of State.

PACS numbers: 95.30.Qd, 95.30.Sf, 04.30.Nk

1 Introduction

The sky is full of fascinating cosmic objects including planets, stars and compact objects like black holes. A black hole is a region of space where the pull of gravity is so strong the even light cannot escape. Black holes are

*msharif@math.pu.edu.pk

described in the framework of relativistic astrophysics. General Relativity leads to insight and understanding of black hole physics.

Rotating black holes exist in the nuclei of galaxies. The gravitational pull of the black hole drags the material (highly magnetized plasma) from nearby stars and forms an accretion disk as it spirals inwards and finally disappears into the black hole. Highly magnetized plasma surrounding the black hole horizon is considered as a magneto-rotational fluid governed by the general relativistic magnetohydrodynamical (GRMHD) equations due to its motion under immense gravity. The magnetohydrodynamical waves produced in these magneto-rotational fluids not only help to confirm the existence of a black hole but also transmit the information inside the magnetosphere. In addition, these show the response of black holes to the external perturbations. The 3+1 ADM formalism [1] is frequently used to discuss the space plasmas into the arena of black holes. Thorne and Macdonald [2]-[4] dealt the electromagnetic fields of the black hole theory with 3+1 formalism. Later, this formalism was used by Holcomb and Tajima [5], Holcomb [6] and Dettmann et al. [7] to study wave propagation in the early universe. Buzzi et al. [8, 9] used the 3+1 GRMHD equations to study one dimensional transverse and longitudinal waves in two-component plasma in the vicinity of the Schwarzschild horizon.

There exists large body of literature [10]-[27] which indicates keen interest in plasmas, plasma processes and plasma waves for the magnetospheres of compact objects. Punsley [10] discussed the electromagnetism and plasma waves created in the ingoing and outgoing perfect MHD ergospheric winds. Beskin et al. [11] gave the comprehensive analysis of the pulsar magnetosphere and discussed the pair creation region around a black hole. Park and Vishniac [12] included the effects of plasma accretion flows on the mass and angular momentum-loss rates in addition to the pure electromagnetic extraction of energy from the rotating black hole. Takahashi et al. [13] focused on the Alfvén surface. By considering the cold limit, trans-Alfvénic solutions are characterized and MHD inflow is discussed in relation to the extraction of energy from the rotating black hole and the accretion of winds or jets.

Ruffini and Wilson [14] proposed the idea of energy extraction from the Kerr black hole. Blandford and Znajek [15] were the first to construct a global model for the magnetosphere of a Kerr black hole in the force-free limit. They demonstrated that energy could be extracted under certain conditions in the form of a Poynting flux. They applied their model to radio loud AGNs, and proposed that extragalactic jets are the consequence of this energy extraction

mechanism [16]. Several authors [17] discussed different aspects of Blandford - Znajek process.

Energy extraction is discussed by different authors [18] assuming the magnetic field lines connected with the transition region instead of connecting with remote loads inside the accretion disk. Zhang [19, 20] formulated the 3+1 black hole theory for stationary symmetric GRMHD and applied it to cold plasma filled Kerr magnetosphere. Using the interface conditions defined at the pair production region, he obtained the numerical solutions which show that outflow of energy flux is possible for the specific angular frequency and specific x -component of the wave vector.

Lee et al. [21]-[23] considered the Blandford-Znajek process as one of the viable models of powering the gamma-ray bursts effectively. The gamma ray bursts is a consequence of interaction of magnetic field and plasma. The observations of a broad Fe $K\alpha$ line in the bright Seyfert 1 galaxy MCG-6-30-15 and M87 [24]-[26] suggest evidences of the extraction of rotational energy from a Kerr black hole by a magnetic field. Thus, the popularity of the GRMHD behavior of plasma has increased and the study of GRMHD waves become more important. Koide et al. [27] discussed plasma flowing into a rapidly rotating black hole by using numerical simulations via GRMHD.

Sharif et al. [28] considered the cold and isothermal plasmas in the vicinity of a Schwarzschild event horizon. Plasma wave properties are investigated using 3+1 formalism. The results are generalized by considering the Schwarzschild geometry as a restricted Kerr model. We [29]-[31] have investigated cold plasma wave properties (real and complex wave numbers) and isothermal plasma wave properties (only real wave numbers) [32] for Kerr planar analogue.

This paper is devoted to discuss the isothermal plasma wave properties by using complex wave numbers. We consider an isothermal plasma in the vicinity of the Kerr magnetosphere's pair production region. The corresponding dispersion relations are obtained by using Fourier analyzed perturbed GRMHD equations. We then evaluate wave numbers which are used to find x -components of propagation and attenuation vectors, phase and group velocities. These quantities help to investigate the properties of plasma.

The organization of the paper is given as follows: Next section provides the background metric with flow assumptions and respective physical interpretation. Section **3** contains the Fourier analyzed GRMHD equations for isothermal plasma in Kerr planar analogue. Section **4** is devoted to the numerical solutions of the dispersion relation including Figures and related

discussion. We shall summarize this discussion in Section 5.

2 3+1 Background and Relative GRMHD Equations

The general line element in ADM 3+1 formalism can be written as [20]

$$ds^2 = -\alpha^2 dt^2 + \eta_{ij}(dx^i + \beta^i dt)(dx^j + \beta^j dt), \quad (2.1)$$

where α is the time lapse and $\bar{\beta}$ is the three-dimensional shift vector and η_{ij} are the components of three-dimensional hypersurface metric. The quantities α , β_i , η_{ij} , ($i, j = 1, 2, 3$) are dependent on coordinates (t, x_i) .

We consider the planar analogue of the Kerr metric (Eq.(2.2) of [32])

$$ds^2 = -dt^2 + (dx + \beta(z)dt)^2 + dy^2 + dz^2. \quad (2.2)$$

Here the lapse function is set to unity and the shift vector β is along x -direction only. The details of the analogue metric are mentioned in Section 2 of [32]. In this planar analogue (Eq.(2.2)), we consider a rotating isothermal plasma admitting the following equation of state

$$\mu = \frac{\rho + p}{\rho_0} = \text{constant}, \quad (2.3)$$

where μ , ρ_0 , ρ and p (all are taken to be constants) are the specific enthalpy, rest and moving mass densities and pressure of the fluid respectively. This highly magnetized plasma includes the effects of gravity (due to nearest correspondence to the black hole). Thus perfect GRMHD equations express it completely.

For the line element given by Eq.(2.1), the perfect GRMHD equations (Maxwell's equations of magnetic field evolution, local conservation laws of mass, momentum and energy in force-free magnetosphere respectively) are [29]

$$\frac{d\mathbf{B}}{d\tau} + \frac{1}{\alpha}\mathbf{B}\cdot\nabla\bar{\beta} + \theta\mathbf{B} = \frac{1}{\alpha}\nabla \times (\alpha\mathbf{V} \times \mathbf{B}), \quad (2.4)$$

$$\frac{D\rho_0}{D\tau} + \rho_0\gamma^2\mathbf{V}\cdot\frac{D\mathbf{V}}{D\tau} + \frac{\rho_0}{\alpha}\left\{\frac{g_{,t}}{2g} + \nabla\cdot(\alpha\mathbf{V} - \bar{\beta})\right\} = 0, \quad (2.5)$$

$$\begin{aligned} & \left\{\left(\rho_0\gamma^2\mu + \frac{\mathbf{B}^2}{4\pi}\right)\eta_{ij} + \rho_0\gamma^4\mu V_i V_j - \frac{1}{4\pi}B_i B_j\right\}\frac{DV^j}{D\tau} + \rho_0\gamma^2 V_i \frac{D\mu}{D\tau} \\ & - \left(\frac{\mathbf{B}^2}{4\pi}\eta_{ij} - \frac{1}{4\pi}B_i B_j\right)V^j{}_{|k}V^k = -\rho_0\gamma^2\mu\left\{a_i - \frac{1}{\alpha}\bar{\beta}_{j|i}V^j - (\mathcal{L}_t\eta_{ij})V^j\right\} \\ & - p_{|i} + \frac{1}{4\pi}(\mathbf{V}\times\mathbf{B})_i\nabla\cdot(\mathbf{V}\times\mathbf{B}) - \frac{1}{8\pi\alpha^2}(\alpha\mathbf{B})^2_{|i} + \frac{1}{4\pi\alpha}(\alpha B_i)_{|j}B^j \\ & - \frac{1}{4\pi\alpha}(\mathbf{B}\times\{\mathbf{V}\times[\nabla\times(\alpha\mathbf{V}\times\mathbf{B}) - (\mathbf{B}\cdot\nabla)\bar{\beta}] \\ & + (\mathbf{V}\times\mathbf{B})\cdot\nabla\bar{\beta}\})_i, \end{aligned} \quad (2.6)$$

$$\begin{aligned} & \frac{d}{d\tau}(\rho_0\mu\gamma^2) - \frac{dp}{d\tau} + \theta\left((\rho_0\mu\gamma^2 - p) + \frac{1}{8\pi}((\mathbf{V}\times\mathbf{B})^2 + \mathbf{B}^2)\right) \\ & + \frac{1}{2\alpha}\{\rho_0\mu\gamma^2 V^i V^j + p\eta^{ij} - \frac{1}{4\pi}((\mathbf{V}\times\mathbf{B})^i(\mathbf{V}\times\mathbf{B})^j + B^i B^j) \\ & + \frac{1}{8\pi}((\mathbf{V}\times\mathbf{B})^2 + \mathbf{B}^2)\eta^{ij}\}\mathcal{L}_t\eta_{ij} + \rho_0\mu\gamma^2\mathbf{V}\cdot\mathbf{a} + \rho_0\mu\gamma^4\mathbf{V}\cdot(\mathbf{V}\cdot\nabla)\mathbf{V} \\ & - \frac{1}{2\pi}\mathbf{a}\cdot((\mathbf{V}\times\mathbf{B})\times\mathbf{B}) - \frac{1}{4\pi}(\nabla\times(\mathbf{V}\times\mathbf{B}))\cdot\mathbf{B} - \frac{1}{\alpha}\{\rho_0\mu\gamma^2\mathbf{V}\cdot(\mathbf{V}\cdot\nabla)\bar{\beta} \\ & + p(\nabla\cdot\bar{\beta}) - \frac{1}{4\pi}(\mathbf{V}\times\mathbf{B})\cdot((\mathbf{V}\times\mathbf{B})\cdot\nabla)\bar{\beta} - \frac{1}{4\pi}\mathbf{B}\cdot(\mathbf{B}\cdot\nabla)\bar{\beta} \\ & + \frac{1}{8\pi}((\mathbf{V}\times\mathbf{B})^2 + \mathbf{B}^2)(\nabla\cdot\bar{\beta})\} + \frac{1}{4\pi}\left(\frac{1}{\alpha}(\mathbf{V}\times\mathbf{B})\cdot\{(\mathbf{V}\times\mathbf{B})\cdot\nabla\}\bar{\beta} \right. \\ & + (\mathbf{V}\times\mathbf{B})\cdot(\mathbf{a}\times\mathbf{B}) + 2(\mathbf{V}\times\mathbf{B})\cdot\frac{d}{d\tau}(\mathbf{V}\times\mathbf{B})\bar{\beta} \\ & \left. + \theta(\mathbf{V}\times\mathbf{B})\cdot(\mathbf{V}\times\mathbf{B}) + \mathbf{B}\cdot\frac{d\mathbf{B}}{d\tau}\right) = 0, \end{aligned} \quad (2.7)$$

where \mathbf{B} , \mathbf{V} , \mathbf{a} respectively denote the three dimensional magnetic field, velocity and acceleration of the fluid, θ gives the expansion of the fluid and $\frac{d}{d\tau}$ is time derivative measured by the fiducial observer, $\frac{D}{D\tau}$ is the time derivative with respect to motion of the fluid, \mathcal{L}_t denotes the Lie derivative with respect to time parameter t . The quantity g is the determinant of the three dimensional hypersurface metric. The respective form of Eqs.(2.4)-(2.7) for the Kerr geometry is given in **Appendix A**.

3 Plasma Discussion and Physical Interpretation

We are going to perform a local analysis to the plasma waves. For this purpose, we have assumed that the plasma living in the spacetime (2.2) admits a free fall along z -direction due to the black hole's gravity and along x -direction due to rotation of the black hole (in direction of shift vector of our analogue spacetime). The fluid's velocity (\mathbf{V}) and magnetic field (\mathbf{B}) measured by our fiducial observer (a natural observer associated with the spacetime and locally measures the quantities) can be described as follows:

$$\mathbf{V} = V(z)\mathbf{e}_x + u(z)\mathbf{e}_z, \quad \mathbf{B} = B\{\lambda(z)\mathbf{e}_x + \mathbf{e}_z\}, \quad (3.1)$$

where B is a constant.

In our stationary symmetric background, the x -component of the velocity vector can be written in the form [20] $V = C + \lambda u$, where $C \equiv \beta + V_F$ with V_F as an integration constant. We assume the value of the shift function [20] $\beta = \tanh(z) - 1$ and $V_F = 1$. Further, $B^2 = 8\pi$ and $\lambda = 1$ are taken so that the magnetic field becomes constant. Thus the x -component takes the form $V = 1 + \beta + u = \tanh(z) + u$. Substituting the value of V in the conservation law of rest-mass for three-dimensional hypersurface, i.e.,

$$\rho_0 \gamma u = \mu(\rho + p) \gamma u = A \text{ (constant)} \quad (3.2)$$

with the assumption that rest-mass density is constant and $A/\rho_0 = 1$, we get an equation of the form

$$3u^2 + 2u \tanh(z) + \tanh^2(z) - 1 = 0$$

quadratic in u . The solutions of this equation (u_1 and u_2) and the corresponding values of V (V_1 and V_2) are given as follows (Eqs.(5.2)-(5.3) of [32]):

$$\left. \begin{aligned} u_1 &= -\frac{1}{3} \tanh(z) - \frac{1}{3} \sqrt{3 - 2 \tanh^2(z)}, \\ V_1 &= \frac{2}{3} \tanh(z) - \frac{1}{3} \sqrt{3 - 2 \tanh^2(z)}, \end{aligned} \right\} \quad (3.3)$$

$$\left. \begin{aligned} u_2 &= -\frac{1}{3} \tanh(z) + \frac{1}{3} \sqrt{3 - 2 \tanh^2(z)}, \\ V_2 &= \frac{2}{3} \tanh(z) + \frac{1}{3} \sqrt{3 - 2 \tanh^2(z)}. \end{aligned} \right\} \quad (3.4)$$

The corresponding Poynting vector (\mathbf{S}) is

$$\mathbf{S} = \frac{1}{4\pi} \mathbf{E} \times \mathbf{B} = 2 \tanh(z)(\mathbf{e}_x - \mathbf{e}_z), \quad (3.5)$$

where \mathbf{E} is the electric field as measured by the fiducial observer. This electric field can be determined by the perfect flow assumption, i.e.,

$$\mathbf{E} = -\mathbf{V} \times \mathbf{B}. \quad (3.6)$$

We have assumed that plasma is produced in the pair production region lying at $z = 0$. A perturbation method is used in which we perturb the equilibrium by a very small amount, for example, the background plasma mass density is not the same as ρ_0 everywhere but changes slightly with $\delta\rho$. The perturbed quantities are assumed to be small and we have considered these as first order quantities. Perturbation assumptions and equations are given in **Appendix A**.

The perturbations are produced due to plasma production in the pair production region. In this region, electron-positron pairs are produced and taken apart by strong forces of gravity. The electrons move towards the outer end of the magnetosphere while the positron move towards the event horizon. Thus the displaced electron results a positive charge density which is produced at the position from where electrons are displaced. These positive charges then attract the electrons. Electrons move back but they overshoot it, and come back but overshoot again and thus oscillation is produced. Same is the case of positrons which produce oscillations in the region towards the event horizon of the black hole.

Here we check the properties of the plasma as a consequence of the plasma perturbations. For this purpose, we have specifically tried to over check the regions in the neighborhood of the pair production region, i.e. $z = 0$. It is important to note that the production of plasma does not make any change in the background geometry. It only disturbs the fluid dynamics. Thus, all geometric terms are considered to 0th order.

4 Fourier Analyzed Perturbed GRMHD Equations

We have assumed that the perturbations produced are simple harmonic waves. We shall discuss the wave properties with the normal mode anal-

ysis (Fourier decomposition of waves). The following assumptions will be used for the sake of Fourier analysis (Eq.(3.3) of [32]).

$$\begin{aligned}
\tilde{\rho}(t, x, z) &= c_1 e^{-i(\omega t - k_x x - k_z z)}, & \tilde{p}(t, x, z) &= c_6 e^{-i(\omega t - k_x x - k_z z)}, \\
v_x(t, x, z) &= c_2 e^{-i(\omega t - k_x x - k_z z)}, & v_z(t, x, z) &= c_3 e^{-i(\omega t - k_x x - k_z z)}, \\
b_x(t, x, z) &= c_4 e^{-i(\omega t - k_x x - k_z z)}, & b_z(t, x, z) &= c_5 e^{-i(\omega t - k_x x - k_z z)}.
\end{aligned} \quad (4.1)$$

Here c_i , ($i = 1, 2, \dots, 6$) are constants, $\mathbf{k} = (k_x, 0, k_z)$ is the wave vector and ω is the angular frequency of the waves.

The wave vector leads to the following quantities:

- $Re(\mathbf{k})$ gives a vector, called propagation vector, that shows three dimensional propagation of waves.
- $Im(\mathbf{k})$ gives a vector, called attenuation vector, that shows damping and growth of waves in three dimensions.
- The phase velocity vector gives the speed of phase in three dimensions and can be calculated by the formula $\frac{\omega}{Re(\mathbf{k})}$.
- The group velocity vector gives the speed of wave packet in three dimensions and can be calculated by the formula $\frac{d\omega}{dRe(\mathbf{k})}$.

We consider the perturbed perfect GRMHD equations written in 3+1 formalism for the Kerr planar analogue with isothermal state of plasma (Eq.(2.3)) given by Eqs.(A13)-(A14). The Fourier analyzed perturbed form of these equations is given as follows (Eqs.(4.6)-(4.12) of [32]):

$$\iota k_z c_2 - (\iota k_z \lambda + \lambda') c_3 - c_4 (\iota k_z u - \iota \omega + u') + c_5 (\vartheta \iota k_z + \vartheta') = 0, \quad (4.2)$$

$$\iota k_x c_2 - \iota k_x \lambda c_3 + \iota c_5 (\vartheta k_x + k_z u - \omega) = 0, \quad (4.3)$$

$$k_x c_4 = -k_z c_5, \quad (4.4)$$

$$\begin{aligned}
& c_1 [\iota \rho (-\omega + \vartheta k_x + u k_z) - (p' u + p u' + p u \gamma^2 \varphi)] + c_2 (\rho + p) \\
& \times [-\eta \gamma^2 V + \iota k_z \gamma^2 u V + \iota k_x \pi + \gamma^2 u \{(\pi + \gamma^2 V^2) V' + 2 \gamma^2 u V u'\}] \\
& + c_3 (\rho + p) \left[-\eta \gamma^2 u + \iota k_x \gamma^2 u V + (\iota k_z - (1 - 2 \gamma^2 u^2) \frac{u'}{u}) \varrho + 2 \gamma^4 u^2 V V' \right] \\
& + c_6 [\iota p (-\omega + \vartheta k_x + u k_z) + (p' u + p u' + p u \gamma^2 \varphi)] = 0, \quad (4.5) \\
& c_1 \rho \gamma^2 u \{ \pi V' + \gamma^2 u V u' \} + c_6 p [\gamma^2 u \{ \pi V' + \gamma^2 u V u' \} + \iota k_x] \\
& + c_2 [-\eta \{ (\rho + p) \gamma^2 \pi + \psi \} + \zeta \{ (\rho + p) \gamma^2 (1 + \gamma^2 V^2) - \psi \}]
\end{aligned}$$

$$\begin{aligned}
& +(\rho + p)\gamma^4 u\{(\pi + 3\gamma^2 V^2)uu' + 4\pi VV'\} + c_3 [-\eta\{(\rho + p)\gamma^4 uV \\
& - \psi\lambda\} + \zeta\{(\rho + p)\gamma^4 uV + \psi\lambda\} + (\rho + p)\gamma^2[2\gamma^2(\varrho + \gamma^2 u^2)uV u' \\
& + \{(\varrho + \gamma^2 u^2)(\pi + \gamma^2 V^2) - \gamma^2 V^2\}V'] + \psi c_4\{-\iota k_z(1 - u^2) \\
& + uu'\} + \psi c_5\{-\lambda' - u\vartheta' + \iota k_x(1 - V^2) - 2\iota uV k_z\} = 0, \tag{4.6}
\end{aligned}$$

$$\begin{aligned}
& c_1\gamma^2\rho[u\{\varrho u' + \gamma^2 V uV'\} - V\beta'] + c_6[\gamma^2 p\{\varrho uu' + \gamma^2 V u^2 V' - V\beta'\} \\
& + p' + p\iota k_z] + c_2 [-\eta\{(\rho + p)\gamma^4 uV - \psi\lambda\} + \zeta\{(\rho + p)\gamma^4 uV \\
& + \psi\lambda\} + (\rho + p)\gamma^2\{\gamma^2 u^2 V'(\pi + 3\gamma^2 V^2) - \beta'(\pi + \gamma^2 V^2) + 2V\gamma^2 uu' \\
& \times (\varrho + \gamma^2 u^2)\}] + c_3 [-\eta\{(\rho + p)\gamma^2 \varrho + \psi\lambda^2\} + \zeta\{(\rho + p)\gamma^2 \varrho - \psi\lambda^2\} \\
& + (\rho + p)\gamma^2[u'(1 + \gamma^2 u^2)(1 + 4\gamma^2 u^2) + 2u\gamma^2\{(\varrho + \gamma^2 u^2)V V' - V\beta'\}] \\
& - \psi\lambda\lambda'u] + \psi c_4\{\iota k_z\lambda(1 - u^2) + \lambda' - \lambda uu'\} + \psi c_5\{2\lambda uV\iota k_z + \lambda u\vartheta' \\
& - \lambda\iota k_x(1 - V^2)\} = 0, \tag{4.7}
\end{aligned}$$

$$\begin{aligned}
& c_1\gamma^2[\rho'u - \rho(\iota\omega + u' + 2u\gamma^2\varphi - \gamma^2 uV\beta' + \iota k_x\vartheta + \iota k_z u)] \\
& + c_6[-\iota\omega p(\gamma^2 - 1) + \gamma^2\{p'u + p(u' + 2u\gamma^2\varphi - \gamma^2 uV\beta' + \iota k_x\vartheta + \iota k_z u)\}] \\
& + c_2[-\iota\omega\{2(\rho + p)\gamma^4 V - \psi\chi\} + \iota k_x[(\rho + p)\gamma^2\{1 + 2\gamma^2 V\vartheta\} - \psi\vartheta\chi] \\
& + \iota k_z u\{2(\rho + p)\gamma^4 V + \psi\chi\} + (\rho + p)\gamma^2 u\{2\gamma^2 V' + 6\gamma^4 V\varphi - \beta'(\pi \\
& + \gamma^2 V^2)\} - \psi\lambda'] + c_3[-\iota\omega\{2(\rho + p)\gamma^4 u + \psi\lambda\chi\} + \iota k_x\vartheta\{2(\rho + p)\gamma^4 u \\
& + \psi\lambda\chi\} + \iota k_z\{(\rho + p)\gamma^2(\varrho + \gamma^2 u^2) - \psi\lambda u\chi\} + (\rho + p)\gamma^2\{-\frac{u'}{u} + 2\gamma^2 uu' \\
& + 6\gamma^4 u^2\varphi + \gamma^2\varphi - V\beta'\varrho\} + \psi\lambda'\{\lambda - u\chi\}] + c_4\psi[u\{\lambda' - \chi u'\} + \iota k_z\chi \\
& \times (1 - u^2)] + c_5\psi\{-\lambda'V + u\chi\vartheta' - \iota k_x\chi(1 - V^2) + 2\iota k_z uV\} = 0. \tag{4.8}
\end{aligned}$$

where $\vartheta = V - \beta$, $\varphi = VV' + uu'$, $\chi = u\lambda - V$, $\psi = \frac{B^2}{4\pi}$, $\varrho = 1 + \gamma^2 u^2$, $\pi = 1 + \gamma^2 V^2$, $\zeta = \iota(k_x V + k_z u)$ and $\eta = \iota(\omega + \beta k_x)$. Here prime denotes the derivative of the quantity with respect to the variable z .

5 Numerical Solutions

Equation (4.4) gives $k_z = -\frac{c_4}{c_5}k_x$ and we will assume $k_z = -k_x$ for the sake of simplicity. Using this relation and the assumptions given in paragraphs 1 and 2 of **Section 3**, we simplify Eqs.(4.2), (4.3), (4.5)-(4.8). To obtain a dispersion relation, we use the method given in [33]. We equate the determinant of the coefficients of constants ($c_1, c_2, c_3, c_4, c_5, c_6$) for Eqs.(4.2), (4.3), (4.5)-(4.8) to zero. It gives an equation of the type

$$\begin{aligned}
& A_1(\omega, z)k_x^6 + A_2(\omega, z)k_x^5 + A_3(\omega, z)k_x^4 + A_4(\omega, z)k_x^3 \\
& + A_5(\omega, z)k_x^2 + A_6(\omega, z)k_x + A_7(\omega, z) = 0,
\end{aligned} \tag{5.1}$$

sextic in k_x which cannot be solved exactly to obtain the values of k_x . Thus we use the software *Mathematica* to solve it by using the fluid flow velocities (3.3 and 3.4). Related Mathematica codes are given in **Appendix B**.

We assume that the pair production region is exactly at $z = 0$. Our region of consideration is $-5 \leq z \leq 5$ for wave analysis. This region is taken only to discuss the waves near the pair production region as much as possible. Since the flow variables have large variations in the region $-1 < z < 1$, we avoid this region and solve the dispersion relation for $-5 \leq z \leq -1$ and $1 \leq z \leq 5$ and thus we have two meshes (just like the near and far zones in em-radiation). The mesh $-5 \leq z \leq -1$ indicates the neighborhood of the pair production region towards the event horizon and the mesh $1 \leq z \leq 5$ represents the neighborhood of the pair production region towards the outer end of the magnetosphere. We deal with each mesh separately. For a numerical solution, we take the step-length 0.2 for z and ω and find the value of k_x at each point (z_i, ω_j) , ($i = 1, \dots, 21$, $j = 1, \dots, 51$) of the mesh.

Our dispersion relation (Eq.(5.9)) leads to six complex values of k_x at each point. Thus $k_x = k_{Rx} + \iota k_{Ix}$. The real part k_{Rx} represents the x -component of the propagation vector which leads to the x -components of the phase and group velocities. The imaginary part k_{Ix} represents the x -component of the attenuation vector. The x -component of the propagation vector gives the x -components of the phase velocity ($v_{px} = \frac{\omega}{k_{Rx}}$) and group velocity ($v_{gx} = \frac{d\omega}{dk_{Rx}}$) of the waves. Each root of the dispersion relation is separated and numerical interpolation is used to estimate the surface. The x -components of the propagation vector, attenuation vector, phase and group velocities can be evaluated from these interpolation functions.

It is mentioned here that we investigate the x -component of the above quantities. The equation $k_x = -k_z$ indicates that the behavior of the z -component of the wave vector is opposite to that of the x -component. If the x -component of the wave is normally dispersed in one region, the z -component is anomalously dispersed and vice versa. When the x -components of the propagation vector, attenuation vector, phase and group velocity vectors increase, their corresponding z -components show a decrease and vice versa. The components of the propagation and attenuation vectors, the

phase and group velocities lead us to the wave behavior of the Kerr black hole magnetosphere and the properties of a Veselago medium.

Here, we give a criteria which is used to discuss the two properties of the medium.

- A medium is a Veselago if the propagation vector is in opposite direction to the Poynting vector [34]. In the usual medium, both these vectors admit same direction.
- If the phase velocity is greater than the group velocity, dispersion of waves is normal, anomalous otherwise [35].

We shall use these facts to infer our results.

We have considered two velocities (given by Eqs.(3.3) and (3.4)) for the rotating plasma. For each velocity, we obtain six complex values of the x -component of the wave vector. For fluid flow with velocity components given by (3.3), Figures **1-6** show the dispersion relations in the neighborhood of the pair production region towards the horizon whereas Figures **7-12** indicate these in the neighborhood of the pair production region towards the outer end of the magnetosphere. For the velocity components given by Eq.(3.4), Figures **13-18** and **19-24**, respectively show the dispersion relations in the neighborhood of the pair production region towards the event horizon and towards the outer end of the magnetosphere. All the Figures have graphs **A**, **B**, **C** and **D** representing the x -components of the propagation and attenuation vectors, phase and group velocities respectively.

In the following, we shall discuss some of the figures which lead to important results. A summary of the discussion of results obtained from the remaining figures is given in the last section.

In Figure **1A**, the x -component of the propagation vector takes negative values in the regions $-5 \leq z \leq -4.598$ and $-4.4 < z \leq -1$ while it has positive values for $-4.598 < z \leq -4.4$. For the region towards the event horizon, the x -component of the Poynting vector, given by Eq.(3.5), admits negative values. When we compare these two, the x -components of the propagation and Poynting vectors turn out to be in the opposite direction for the region $-4.598 < z \leq -4.4$ and thus the medium is a Veselago. Figure **1B** indicates that the x -component of the attenuation vector increases with the increase in angular frequency and decreases in z in the region $-2.0 \leq z \leq -1.0$, $0.175 \leq \omega \leq 10$. This shows damping of waves

with increase in angular frequency and wave growth with increase in z . The remaining region shows random damping and growth of waves.

Similarly, in Figure **7A**, the x -component of the propagation vector is negative throughout the region. The x -component of the Poynting vector, given by Eq.(3.5), admits positive values for the region away from the event horizon. The opposite direction of the x -components of the propagation and the Poynting vectors indicates the presence of a Veselago medium.

Table 1 gives the figures along with the region where we have found a Veselago medium, i.e., the the propagation vector is in opposite direction to the attenuation vector.

The negative phase velocity propagation is a property of the usual medium as well as Veselago medium. In this medium, the right hand rule of electromagnetism changes into the left hand rule. This medium has been demonstrated experimentally [36] (the material formed is called left-handed material or meta-material) and is characterized by simultaneous negative magnetic permeability and electric permittivity. It has Poynting vector of a time-harmonic plane wave directed opposite with respect to the wave vector. This exhibits unusual properties like support of backward waves and anomalous negative refraction of plane monochromatic electromagnetic waves. Thus, backward waves are supported by the plasma in these regions.

Figures **1C** and **1D** indicate that the x -component of the group velocity is greater than the phase velocity in the region $-1.75 \leq z \leq -1.0$, $0.5 \leq \omega \leq 10$ which shows anomalous dispersion of waves. Rest of the region admits random points of normal and anomalous dispersion of waves. Table 2 contains figures with regions of the normal dispersion of waves. The regions of normal dispersion indicates that the waves can pass through them without any restriction. Thus the energy flux can pass through these regions (via waves).

6 Summary

This paper is devoted to discuss the properties of isothermal plasma waves by using the perturbed GRMHD equations in 3+1 formalism. These non-linear ordinary differential equations are simplified by using the Fourier decomposition of waves (Fourier analysis of waves). We have computed the dispersion relation for the sinusoidal waves and solved it to check the properties of the medium. This has been done in the neighborhood of the pair production

Figure	Regions of Veselago Medium
2A	$-1.8 \leq z \leq -1$
3A	$-2.05 \leq z \leq -1.0$
4A	$-2.1 \leq z \leq -1.0$
5A	$-5 \leq z \leq -1$
6A	$-5 \leq z \leq -4.6$ and $-4.375 \leq z \leq -1$
8A	$1 \leq z \leq 5$
14A, 15A, 16A, 17A and 18A	$-5 \leq z \leq -1$
19A	$0 < z \leq 4.425$ and $4.585 < z \leq 5$
24A	$4.42 < z \leq 4.595$

Table 1: Regions admitting a Veselago medium in respective figures

Figure	Regions of Normal Dispersion
2C and 2D	$-1.8 \leq z \leq -1.0$
7C and 7D	$1 \leq z \leq 5$
8C and 8D	$0.5 < \omega \leq 5$
10C and 10D	$0.15 \leq \omega \leq 10$
12C and 12D	$1 \leq z \leq 5, 0.3 \leq \omega \leq 0.401$
13C and 13D	$0.1 \leq \omega \leq 0.5$
14C and 14D	$0 \leq \omega < 0.5$
15C and 15D	Except for negligible angular frequency
16C and 16D	$-5.0 \leq z \leq -1.025, 0.4 \leq \omega \leq 10$
18C and 18D	$1.01 \leq \omega \leq 2$
19C and 19D	$1 \leq z \leq 2, 0 < \omega \leq 10$ and $2 \leq z \leq 2.8, 0.75 \leq \omega \leq 10$
20C and 20D	$1 \leq z \leq 1.8, 0.5 \leq \omega \leq 10$

Table 2: Regions of normal dispersion of waves in respective figures

region of the Kerr magnetosphere.

A dispersion relation is found by using *Mathematica* and wave numbers are deduced in terms of angular frequency. The real part of the x -component of the wave vector gives the x -component of the phase and group velocities which lead to the properties of plasma. The imaginary part of the x -component of the wave vector indicates the x -component of the attenuation vector. All these quantities are shown in the graphs.

The following two objectives are investigated in this work:

1. The behavior of GRMHD waves under the influence of gravity and magnetospheric wind is analyzed (especially dispersion of waves is considered). This helps us to detect whether the extraction of energy is possible from the black hole.
2. The existence of a Veselago medium in the black hole regime is checked.

To obtain these objectives, we considered two values of the flow velocity. The dispersion relations for each velocity are calculated and complex x -component of the wave vectors are evaluated by using the relation $k_x = -k_z$. This relation gives us the z -component of the wave vector dependent upon the x -component. The direction of the Poynting and the wave vectors in the region gives an estimate of the refractive index (positive if both have the same direction and negative if both have the opposite direction). The effect of rotation of the black hole yields k_x and the gravitational effect gives k_z . The results can be summarized as follows:

In Figure 1, the medium is usual near the pair production region and shows anomalous dispersion for most of the part. Figure 2 indicates that normal dispersion of waves occurs in a Veselago medium near the pair production region. Figure 3 shows random points of normal and anomalous dispersion in a Veselago medium living near the pair production region. Figure 4 shows that there exists a Veselago medium with random normal and anomalous points of dispersion. In Figure 5, a Veselago medium is found with random points of normal and anomalous dispersion in the neighborhood of the pair production region. Figure 6 shows that there exists a Veselago medium near the pair production region. Random points of normal and anomalous dispersion are found away from the pair production region.

Figure 7 indicates the presence of a Veselago medium along with the normal dispersion of waves. Figure 8 represents most of the region admitting normal dispersion for the waves with high frequencies in a Veselago

medium. In Figure 9, anomalous dispersion of waves in a usual medium is found throughout the region whereas Figure 10 shows that the waves with higher angular frequency are normally dispersed in a usual medium. Figure 11 represents a usual medium admitting anomalous dispersion of waves in most of the region. In Figure 12, small regions admitting normal dispersion of waves are found in usual medium.

In Figure 13, a very small region shows normal dispersion of waves in usual medium. In Figure 14, presence of a Veselago medium is confirmed. Normal dispersion occurs for the waves with low angular frequency, anomalous otherwise. A Veselago medium admitting normal dispersion, except for low frequency waves, is found in Figure 15. In Figure 16, a Veselago medium exists throughout the region. Moreover, a small region near the pair production region admits anomalous dispersion. Most of the region shows normal dispersion. Figure 17 indicates anomalous dispersion of waves in a Veselago medium for most of the region. In Figure 18 random points of normal and anomalous dispersion are found in a Veselago medium.

In Figure 19, a large and a small region exhibit the properties of a Veselago medium. Moreover, near the pair production region normal dispersion of waves exists. Figure 20 shows that most of the region near the pair production region admits normal dispersion of waves in a usual medium. In Figure 21, random points of normal and anomalous dispersion are found. Further, small regions of a Veselago medium are present. In Figure 22, we obtain the usual medium near the pair production region. Random points of normal and anomalous dispersion are found. Figure 23 indicates that the medium is usual admitting anomalous dispersion of waves near the pair production region. Figure 24 shows anomalous dispersion of waves in the usual medium near the pair production region.

From the Figure analysis, we arrive at the following conclusions.

1. We can conclude that the magnetosphere allows the waves to disperse normally towards the event horizon as well as the outer end of the magnetosphere. Thus negative energy flux can fall inside the black hole and rotational energy can be extracted in response.
2. It does not matter whether the region lies towards the event horizon or towards the outer end of the magnetosphere, the presence of a Veselago medium only depends on the rotation of the background.

When we compare the results with the previous literature, we obtain the

following:

- On comparing our results with [31], only Figures 7 and 14 show that energy can be extracted by inflow of negative energy influx. In this work, we have obtained Figures 15, 7, 10 and 20 which show normal dispersion of waves. This indicates that there are more chances of waves to move towards the outer end of the magnetosphere (Figures 7, 10 and 20). Consequently there are more chances of the extraction of energy.
- Here we obtain clear cut conditions to show that extraction of energy is possible. In [32], only inflow of the waves towards the event horizon is possible and their outflow towards the outer end of the magnetosphere is not possible. Thus the exchange of energy from the event horizon with the accreting material was expected to be allowed. However, here we have obtained clear evidences that the energy can be extracted from the event horizon, passes through the accretion disk and can move towards the outer end of the magnetosphere as given by observational identifications in [24]-[26]. This does not negate the work given in [32], but generalizes that idea.

Acknowledgment

We appreciate the Higher Education Commission Islamabad, Pakistan, for its financial support during this work through the *Indigenous PhD 5000 Fellowship Program Batch-II*. Fruitful discussion with Prof. Asghar Qadir is also appreciated.

Appendix A

This Appendix includes the GRMHD equations and their perturbed form by using some assumptions. The component form of these equations is also given.

The set of perfect GRMHD equations for isothermal plasma living in Kerr planar analogue (with rotation assumed to be along x-direction) can be written as (Eqs.(4.1)-(4.5) of [32])

$$\frac{d\mathbf{B}}{d\tau} + (\mathbf{B} \cdot \nabla)\beta = \nabla \times (\mathbf{V} \times \mathbf{B}), \quad (\text{A1})$$

$$\nabla \cdot \mathbf{B} = 0, \quad (\text{A2})$$

$$\frac{D(\rho + p)}{D\tau} + (\rho + p)\gamma^2 \mathbf{V} \cdot \frac{D\mathbf{V}}{D\tau} + (\rho + p)\nabla \cdot \mathbf{V} = 0, \quad (\text{A3})$$

$$\left[\left\{ (\rho + p)\gamma^2 + \frac{\mathbf{B}^2}{4\pi} \right\} \delta_{ij} + (\rho + p)\gamma^4 V_i V_j - \frac{1}{4\pi} B_i B_j \right] \frac{dV^j}{d\tau} + (\rho + p)\gamma^2 V_{i,k} V^k + (\rho + p)\gamma^4 V_i V_j V^j_{,k} V^k = (\rho + p)\gamma^2 \beta_{j,i} V^j - p_{,i} + \frac{1}{4\pi} (B_{i,j} - B_{j,i}) B^j - \frac{1}{4\pi} \left\{ \mathbf{B} \times \left(\mathbf{V} \times \frac{d\mathbf{B}}{d\tau} \right) \right\}_i, \quad (\text{A4})$$

$$\gamma^2 \mathbf{V} \cdot \frac{D}{D\tau} (\rho + p) + 2(\rho + p)\gamma^4 \mathbf{V} \cdot \frac{D\mathbf{V}}{D\tau} - \frac{dp}{d\tau} + (\rho + p)\gamma^2 (\nabla \cdot \mathbf{V}) - (\rho + p)\gamma^2 \mathbf{V} \cdot (\mathbf{V} \cdot \nabla)\beta + \frac{1}{4\pi} [(\mathbf{V} \times \mathbf{B}) \cdot (\nabla \times \mathbf{B}) + (\mathbf{V} \times \mathbf{B}) \cdot \frac{d}{d\tau} (\mathbf{V} \times \mathbf{B}) + (\mathbf{V} \times \mathbf{B}) \cdot \{(\mathbf{V} \times \mathbf{B}) \cdot \nabla\} \beta] = 0, \quad (\text{A5})$$

with \mathbf{V} , \mathbf{B} and \mathbf{E} are fiducial observer (FIDO) measured fluid velocity, magnetic and electric fields respectively, $\frac{d}{d\tau} \equiv \frac{\partial}{\partial t} - \beta \cdot \nabla$ is the FIDO measured rate of change of any three-dimensional vector in absolute space, γ is the

Lorentz factor and $\frac{D}{D\tau} \equiv \frac{d}{d\tau} + \mathbf{V} \cdot \nabla = \frac{\partial}{\partial t} + (\mathbf{V} - \beta) \cdot \nabla$ is the time derivative moving along the fluid.

The perturbed variables take the following form

$$\begin{aligned} \rho &= \rho^0 + \rho\tilde{\rho}, & p &= p^0 + p\tilde{p}, \\ \mathbf{V} &= \mathbf{V}^0 + \mathbf{v}, & \mathbf{B} &= \mathbf{B}^0 + B\mathbf{b}, \end{aligned} \quad (\text{A6})$$

where the dimensionless perturbed quantities are

$$\begin{aligned} \tilde{\rho} &\equiv \frac{\delta\rho}{\rho} = \tilde{\rho}(t, x, z), & \tilde{p} &\equiv \frac{\delta p}{p} = \tilde{p}(t, x, z), \\ \mathbf{v} &\equiv \delta\mathbf{V} = v_x(t, x, z)\mathbf{e}_x + v_z(t, x, z)\mathbf{e}_z, \\ \mathbf{b} &\equiv \frac{\delta\mathbf{B}}{B} = b_x(t, x, z)\mathbf{e}_x + b_z(t, x, z)\mathbf{e}_z. \end{aligned} \quad (\text{A7})$$

When we introduce the perturbations from Eq.(A6), the linearized GRMHD Eqs.(A1)-(A5) become

$$\left\{ \left(\frac{\partial}{\partial t} - \beta \cdot \nabla \right) (\delta\mathbf{B}) \right\} = \nabla \times (\mathbf{v} \times \mathbf{B}) + \nabla \times (\mathbf{V} \times \delta\mathbf{B}) - (\delta\mathbf{B} \cdot \nabla)\beta, \quad (\text{A8})$$

$$\nabla \cdot (\delta\mathbf{B}) = 0, \quad (\text{A9})$$

$$\begin{aligned} &\left\{ \frac{\partial}{\partial t} + (\mathbf{V} - \beta) \cdot \nabla \right\} (\delta\rho + \delta p) + (\rho + p)\gamma^2 \mathbf{V} \cdot \left\{ \frac{\partial}{\partial t} + (\mathbf{V} - \beta) \cdot \nabla \right\} \mathbf{v} \\ &+ (\rho + p)(\nabla \cdot \mathbf{v}) + (\delta\rho + \delta p)(\nabla \cdot \mathbf{V}) + (\delta\rho + \delta p)\gamma^2 \mathbf{V} \cdot (\mathbf{V} \cdot \nabla) \mathbf{V} \\ &= -2(\rho + p)\gamma^2 (\mathbf{V} \cdot \mathbf{v})(\mathbf{V} \cdot \nabla) \ln \gamma - (\rho + p)\gamma^2 (\mathbf{V} \cdot \nabla \mathbf{V}) \cdot \mathbf{v} \\ &+ (\rho + p)\mathbf{v} \cdot \nabla \ln u, \end{aligned} \quad (\text{A10})$$

$$\begin{aligned} &\left[\left\{ (\rho + p)\gamma^2 + \frac{\mathbf{B}^2}{4\pi} \right\} \delta_{ij} + (\rho + p)\gamma^4 V_i V_j - \frac{1}{4\pi} B_i B_j \right] \left(\frac{\partial}{\partial t} - \beta \cdot \nabla \right) v^j \\ &+ (\rho + p)\gamma^2 v_{i,j} V^j + (\rho + p)\gamma^4 V_i v_{j,k} V^j V^k + \frac{1}{4\pi} \left[\mathbf{B} \times \left\{ \mathbf{V} \times \frac{d(\delta\mathbf{B})}{d\tau} \right\} \right]_i \\ &- \frac{1}{4\pi} \{ (\delta B_i)_{,j} - (\delta B_j)_{,i} \} B^j = -(\delta p)_{,i} + \gamma^2 [(\delta\rho + \delta p)V^j \\ &+ 2(\rho + p)\gamma^2 (\mathbf{V} \cdot \mathbf{v})V^j + (\rho + p)v^j] \beta_{j,i} + \frac{1}{4\pi} (B_{i,j} - B_{j,i}) \delta B^j \\ &- (\rho + p)\gamma^4 (v_i V^j + v_j V^i) V_{k,j} V^k - \gamma^2 \{ (\delta\rho + \delta p)V^j \\ &+ 2(\rho + p)\gamma^2 (\mathbf{V} \cdot \mathbf{v})V^j + (\rho + p)v^j \} V_{i,j} - \gamma^4 V_i \{ (\delta\rho + \delta p)V^j \\ &+ 4(\rho + p)\gamma^2 (\mathbf{V} \cdot \mathbf{v})V^j + (\rho + p)v^j \} V_{j,k} V^k, \end{aligned} \quad (\text{A11})$$

$$\begin{aligned}
& \gamma^2 \left\{ \frac{\partial}{\partial t} + (\mathbf{V} - \beta) \cdot \nabla \right\} (\delta\rho + \delta p) + 2(\rho + p)\gamma^4 \mathbf{V} \cdot \left\{ \frac{\partial}{\partial t} \right. \\
& + (\mathbf{V} - \beta) \cdot \nabla \left. \right\} \mathbf{v} - (\rho + p)\gamma^2 \mathbf{v} \cdot \nabla \ln u + (\rho + p)\gamma^4 \mathbf{V} \cdot (\mathbf{v} \cdot \nabla) \mathbf{V} \\
& + 6(\rho + p)\gamma^6 (\mathbf{V} \cdot \mathbf{v}) \mathbf{V} \cdot (\mathbf{V} \cdot \nabla) \mathbf{V} + 2(\delta\rho + \delta p)\gamma^4 \mathbf{V} \cdot (\mathbf{V} \cdot \nabla) \mathbf{V} \\
& + 2(\rho + p)\gamma^4 \mathbf{v} \cdot (\mathbf{V} \cdot \nabla) \mathbf{V} - 2(\rho + p)\gamma^4 (\mathbf{V} \cdot \mathbf{v}) \mathbf{V} \cdot \nabla \ln u + 2(\rho + p)\gamma^4 \\
& \times (\mathbf{V} \cdot \mathbf{v}) (\nabla \cdot \mathbf{V}) - \frac{\partial}{\partial t} (\delta p) + (\delta\rho + \delta p)\gamma^2 (\nabla \cdot \mathbf{V}) + (\rho + p)\gamma^2 (\nabla \cdot \mathbf{v}) \\
& - \gamma^2 (\beta \cdot \nabla) (\delta\rho + \delta p) + 2(\rho + p)\gamma^4 (\mathbf{V} \cdot \mathbf{v}) (\beta \cdot \nabla \ln u) - 6(\rho + p) \\
& \times \gamma^6 (\mathbf{V} \cdot \mathbf{v}) \mathbf{V} \cdot (\beta \cdot \nabla) \mathbf{V} - 2(\rho + p)\gamma^4 \mathbf{v} \cdot (\beta \cdot \nabla) \mathbf{V} - 2(\delta\rho + \delta p)\gamma^4 \mathbf{V} \cdot (\beta \cdot \nabla) \mathbf{V} \\
& - (\delta\rho + \delta p)\gamma^2 \mathbf{V} \cdot (\mathbf{V} \cdot \nabla) \beta - (\rho + p)\gamma^2 \mathbf{V} \cdot (\mathbf{v} \cdot \nabla) \beta \\
& - 2(\rho + p)\gamma^4 (\mathbf{V} \cdot \mathbf{v}) \mathbf{V} \cdot (\mathbf{V} \cdot \nabla) \beta + \frac{1}{4\pi} [(\mathbf{v} \times \mathbf{B}) \cdot (\nabla \times \mathbf{B}) \\
& + (\mathbf{V} \times \delta \mathbf{B}) \cdot (\nabla \times \mathbf{B}) + (\mathbf{V} \times \mathbf{B}) \cdot (\nabla \times \delta \mathbf{B}) \\
& + (\mathbf{V} \times \mathbf{B}) \cdot \left\{ \frac{d\mathbf{v}}{d\tau} \times \mathbf{B} + \mathbf{V} \times \frac{d\delta \mathbf{B}}{d\tau} \right\}] = 0. \tag{A12}
\end{aligned}$$

These equations show the change in the behavior of moving mass, velocity and magnetic field of the fluid when the perturbations are involved. The component form of Eqs.(A8)-(A9) are given as follows.

$$\frac{db_x}{d\tau} + Vb_{x,x} + ub_{x,z} = -u'b_x + v'b_z + v_{x,z} - \lambda v_{z,z} - \lambda'v_z, \tag{A13}$$

$$\frac{db_z}{d\tau} + Vb_{z,x} + ub_{z,z} = \lambda v_{z,x} - v_{x,x}, \tag{A14}$$

$$b_{x,x} + b_{z,z} = 0, \tag{A15}$$

$$\begin{aligned}
& \rho \frac{d\tilde{\rho}}{d\tau} + p \frac{d\tilde{p}}{d\tau} + \rho V \tilde{\rho}_{,x} + p V \tilde{p}_{,x} + \rho u \tilde{\rho}_{,z} + p u \tilde{p}_{,z} - (\tilde{\rho} - \tilde{p}) \{p'u + pu' \\
& + pu\gamma^2(\varphi)\} + (\rho + p)\gamma^2 \left(V \frac{dv_x}{d\tau} + u \frac{dv_z}{d\tau} \right) + (\rho + p) \{ \pi v_{x,x} + \varrho v_{z,z} \\
& + uV\gamma^2(v_{x,z} + v_{z,x}) \} = -(\rho + p)\gamma^2 u [(\pi + \gamma^2 V^2)V' + 2\gamma^2 u V u'] v_x \\
& + (\rho + p) [(1 - 2\gamma^2 u^2) \varrho \frac{u'}{u} - 2\gamma^4 u^2 V V'] v_z, \tag{A16}
\end{aligned}$$

$$\begin{aligned}
& \{(\rho + p)\gamma^2 \pi + \psi\} \frac{dv_x}{d\tau} + \{(\rho + p)\gamma^4 u V - \psi \lambda\} \frac{dv_z}{d\tau} - 2\psi u V b_{z,z} \\
& + \{(\rho + p)\gamma^2 \pi - \psi\} (V v_{x,x} + u v_{x,z}) + \{(\rho + p)\gamma^4 u V + \psi \lambda\} \\
& \times (V v_{z,x} + u v_{z,z}) + \psi \{ (1 - V^2) b_{z,x} - (1 - u^2) b_{x,z} \} = -\psi u u' b_x \\
& + \psi \{ \lambda' + u v' \} b_z - p \tilde{p}_{,x} - (\rho \tilde{\rho} + p \tilde{p}) \gamma^2 u \{ (1 + \gamma^2 V^2) V' + \gamma^2 u V u' \}
\end{aligned}$$

$$\begin{aligned}
& -(\rho + p)\gamma^4 u \{(1 + 4\gamma^2 V^2)uu' + 4\pi VV'\}v_x - [(\rho + p)\gamma^2 \\
& \times \{(1 + 2\gamma^2 u^2)(1 + 2\gamma^2 V^2) - \gamma^2 V^2\}V' \\
& + 2\gamma^2(1 + 2\gamma^2 u^2)uV u'] + \psi u \lambda' v_z, \tag{A17}
\end{aligned}$$

$$\begin{aligned}
& \{(\rho + p)\gamma^2 \varrho + \psi \lambda^2\} \frac{dv_z}{d\tau} + \{(\rho + p)\gamma^4 uV - \psi \lambda\} \frac{dv_x}{d\tau} \\
& + \{(\rho + p)\gamma^2 \varrho - \psi \lambda^2\} (Vv_{z,x} + uv_{z,z}) + 2\psi \lambda u V b_{z,z} \\
& + \{(\rho + p)\gamma^4 uV + \psi \lambda\} (Vv_{x,x} + uv_{x,z}) - \psi \lambda \{(1 - V^2)b_{z,x} \\
& - (1 - u^2)b_{x,z}\} = -\psi(\lambda' - \lambda uu')b_x - \psi \lambda u \vartheta' b_z - \rho \tilde{\rho} \gamma^2 \{uu' \varrho \\
& + \gamma^2 u^2 VV' - V\beta'\} - [p\tilde{p}_{,z} + p'\tilde{p} + p\tilde{p}\gamma^2 \{uu' \varrho + \gamma^2 u^2 VV' - V\beta'\}] \\
& - (\rho + p)\gamma^2 [\gamma^2 u^2 (1 + 4\gamma^2 V^2)V' - (1 + 2\gamma^2 V^2)\beta' \\
& + 2\gamma^2 uV(1 + 2\gamma^2 u^2)u']v_x - [(\rho + p)\gamma^2 \{-2\gamma^2 uV\beta' + \varrho(1 + 4\gamma^2 u^2)u' \\
& + 2\gamma^2(\varrho + \gamma^2 u^2)uVV'\} - \psi \lambda u \lambda']v_z, \tag{A18}
\end{aligned}$$

$$\begin{aligned}
& \gamma^2 \rho \frac{\partial \tilde{\rho}}{\partial t} + p(\gamma^2 - 1) \frac{\partial \tilde{p}}{\partial t} + \tilde{p}\gamma^2 \{\rho' u + \rho u' + 2\rho u \gamma^2 \varphi - \rho u V \beta'\} + \gamma^2 \rho \tilde{\rho}_{,x} \vartheta \\
& + \gamma^2 u \rho \tilde{\rho}_{,z} + \tilde{p}\gamma^2 \{u p' + u' p + 2p u \gamma^2 \varphi - p \gamma^2 u V \beta'\} + \gamma^2 p \tilde{p}_{,x} \vartheta + \gamma^2 u p \tilde{p}_{,z} \\
& + \frac{\partial v_x}{\partial t} \{2(\rho + p)\gamma^4 V - \psi \chi\} + \frac{\partial v_z}{\partial t} \{2(\rho + p)\gamma^4 u + \psi \lambda \chi\} \\
& + v_{x,x} [(\rho + p)\gamma^2 \{1 + 2\gamma^2 V \vartheta\} - \psi \vartheta \chi] + v_{x,z} u [2(\rho + p)\gamma^4 V + \psi \chi] \\
& + v_{z,x} \vartheta [2(\rho + p)\gamma^4 u + \psi \lambda \chi] + v_{z,z} \{(\rho + p)(\varrho + \gamma^2 u^2) - \psi \lambda u \chi\} \\
& + \psi \chi \{(1 - u^2)b_{x,z} - (1 - V^2)b_{z,x} + 2uV b_{z,z}\} \\
& + \psi u b_x (\lambda' - \chi u') + \psi b_z (-\lambda' V + u \chi \vartheta') + v_x [(\rho + p)\gamma^2 u \{2\gamma^2 V' \\
& + 6\gamma^4 V \varphi - \beta'(\pi + \gamma^2 V^2)\} - \psi \lambda'] + v_z [\psi \lambda' (\lambda - u \chi) \\
& + (\rho + p)\gamma^2 \{-\frac{u'}{u} + 2\gamma^2 uu' + 6\gamma^4 u^2 \varphi + \gamma^2 \varphi - V\beta' \varrho\}] = 0. \tag{A19}
\end{aligned}$$

We have used the conservation law of rest-mass for three-dimensional hypersurface given by Eq.(3.2) to simplify Eq.(A16).

Appendix B

Here we include the *Mathematica* program used to calculate a dispersion relation. This dispersion relation is obtained from the real part of the determinant.

In the start, we must specify relative assumptions given in Section 3 to simplify the dispersion relations. In the following, we only consider the veloc-

the replacement of $\{z, -5, -1, 0.2\}$ by $\{z, 1, 5, 0.2\}$ can be used to calculate the roots for the region away from the event horizon. The commands are given as follows:

```
R = NSolve[b == 0, k];
```

```
Table[{z, ω, Part[R, 1]}, {z, -5, -1, 0.2}, {ω, 0, 10, 0.2}]
Table[{z, ω, Part[R, 2]}, {z, -5, -1, 0.2}, {ω, 0, 10, 0.2}]
Table[{z, ω, Part[R, 3]}, {z, -5, -1, 0.2}, {ω, 0, 10, 0.2}]
Table[{z, ω, Part[R, 4]}, {z, -5, -1, 0.2}, {ω, 0, 10, 0.2}]
Table[{z, ω, Part[R, 5]}, {z, -5, -1, 0.2}, {ω, 0, 10, 0.2}]
```

Afterwards, each root is separated in the form of arrays for further manipulation. Each root is approximated for each point of the two-dimensional meshes $-5 \leq z \leq -1$, $0 \leq \omega \leq 10$ and $1 \leq z \leq 5$, $0 \leq \omega \leq 10$, with equal step lengths 0.2 for z and ω . The numerical values in each region are used to approximate interpolation functions.

The data for each root is converted and separately dealt in Mathematica by the following commands. The graph of the root admitting real values at each point of the mesh can be generated by the following procedure to obtain Figure 1 (e.g.).

```
datapts = {{a11, a12, ..., a1 51}, {a21, a22, ..., a2 51}, ..., {a26 1, a26 2, ..., a26 51}};
```

```
r = ListInterpolation[datapts, {{-5, -1}, {0, 10}}]
```

```
p = Re[r[x, y]];
```

```
q = Im[r[x, y]];
```

```
p1 = Plot3D[p, {z, -5, -1}, {ω, 0, 10}, AxesLabel → {"z", "ω", " "}]
```

```
p2 = Plot3D[q, {z, -5, -1}, {ω, 0, 10}, AxesLabel → {"z", "ω", " "}]
```

```
p3 = Plot3D[ $\frac{y}{p}$ , {z, -5, -1}, {ω, 0, 10}, AxesLabel → {"z", "ω", " "}]
```

```
l = D[r[x, y], y];
```

p4 = Plot3D[$\frac{1}{\text{Re}[\]}$, {z, -5, -1}, { ω , 0, 10}, AxesLabel \rightarrow {"z", " ω ", " "}]

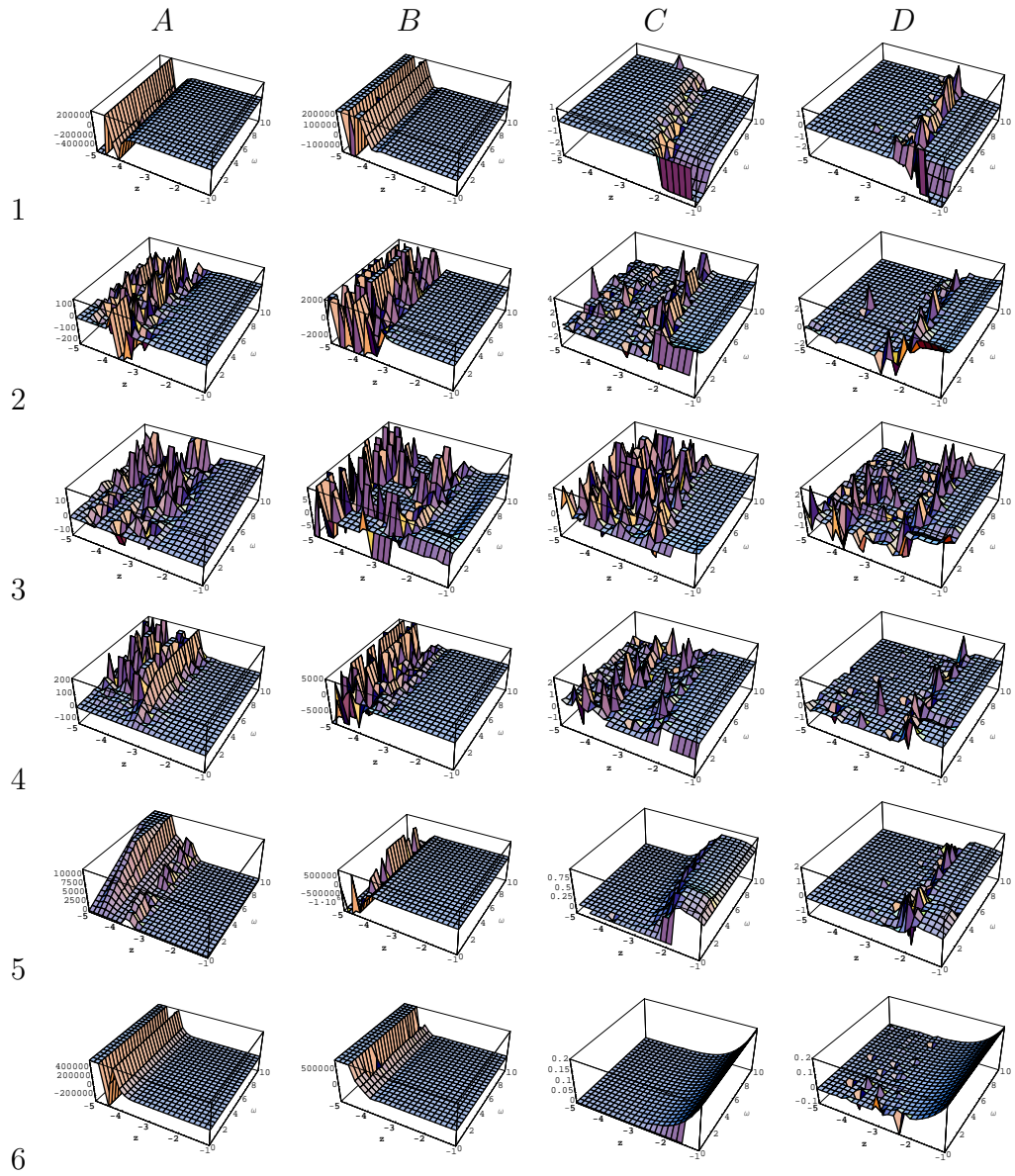
These commands generate x -components of the propagation and attenuation vectors, phase and group velocities for the specific set of data points in the form of graphs. These graphs are used to investigate the properties of the medium.

References

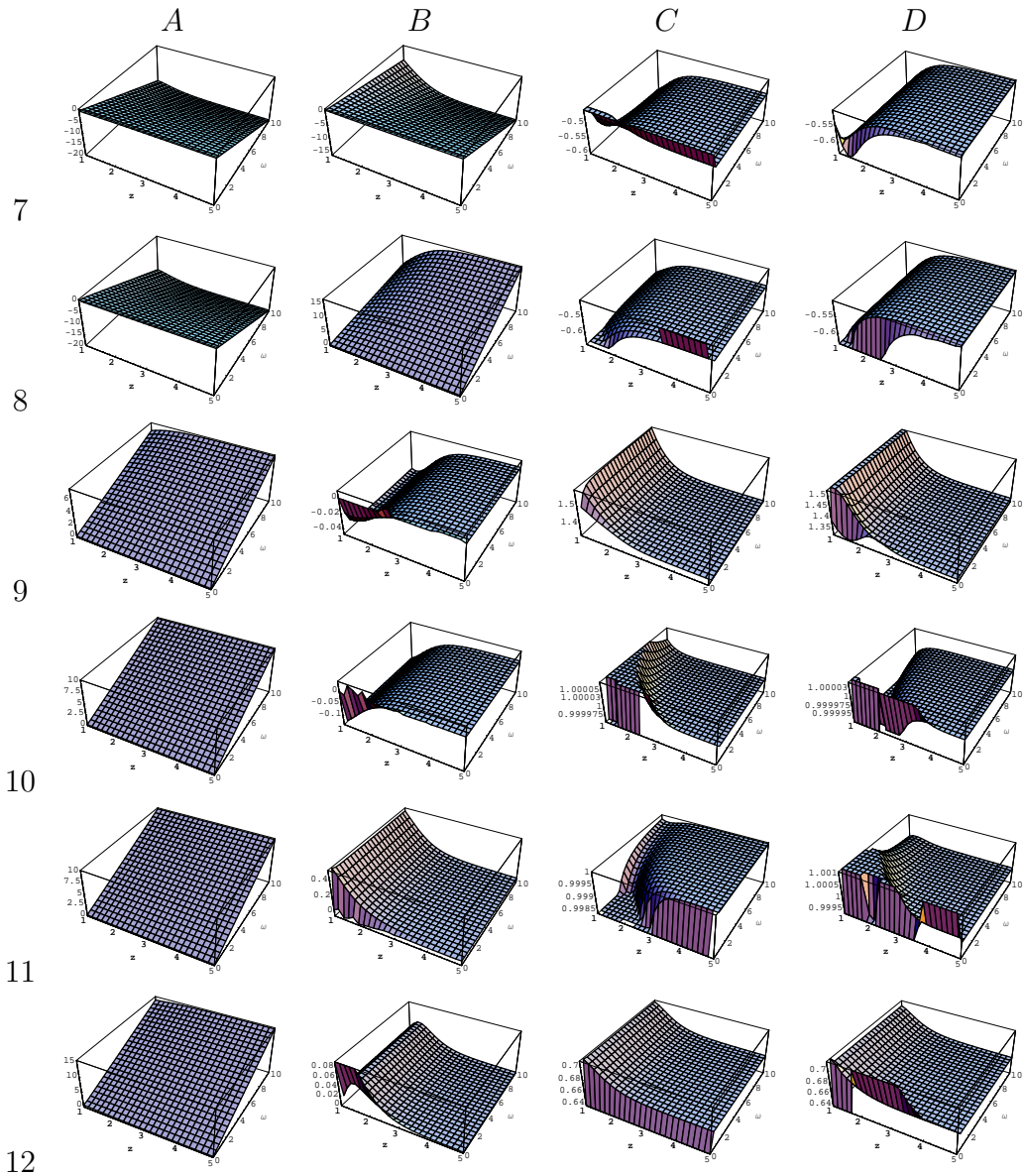
- [1] Arnowitt, R., Deser, S. and Misner, C.W.: *Gravitation: An Introduction to Current Research* (Wiley, New York, 1962).
- [2] Thorne, K.S. and Macdonald, D.A.: Mon. Not. R. Astr. Soc. **198**(1982)339.
- [3] Thorne, K.S. and Macdonald, D.A.: Mon. Not. R. Astr. Soc. **198**(1982)345.
- [4] *Black Holes: The Membrane Paradigm*, eds. Thorne, K.S., Price, R.H. and Macdonald, D.A., (Yale University Press, New Haven, 1986).
- [5] Holcomb, K.A. and Tajima, T.: Phys. Rev. **D40**(1989)3809.
- [6] Holcomb, K.A.: Astrophys. J. **362**(1990)381.
- [7] Dettman, C.P., Frankel, N.E. and Kowalenko, V.: Phys. Rev. **D48**(1993)5655.
- [8] Buzzi, V., Hines, K.C. and Treumann, R.A.: Phys. Rev. **D51**(1995)6663.
- [9] Buzzi, V., Hines, K.C. and Treumann, R.A.: Phys. Rev. **D51**(1995)6677.
- [10] Punsly, B.: *Black Hole Gravitohydromagnetics* (Springer-Verlag Berlin, 2001).
- [11] Beskin, V.S., Gurevich, A.V. and Istomin, Y. N.: *Physics of the Pulsar Magnetosphere* (Cambridge University Press, 1993).

- [12] Park, S.J. and Vishniac, E.T.: *Astrophys. J.* **332**(1988)135.
- [13] Takahashi, M., Nitta, S., Tatematsu, Y. and Tomimatsu, A.: *Astrophys. J.* **363**(1990)206.
- [14] Ruffini, R. and Wilson, J.R.: *Phys. Rev.* **D12**(1975)2959.
- [15] Blandford, R.D. and Znajek, R.L.: *Mon. Not. Roy. Astron. Soc.* **179**(1977)433.
- [16] Begelman, M.C.; Blandford, R.D.; Rees, M.J. *Rev. Mod. Phys.* **56** (1984)255.
- [17] Romanova, L.L. and Lovelace, R.V.E.: *Astron. Astrophys.* **262**(1992)26;
 Romanova, L.L. and Lovelace, R.V.E.: *Astrophys. J.* **457**(1997)97;
 Levinson, A. and Blandford, R.D.: *Astrophys. J.* **456**(1996)L29;
 Mannheim, K.: *Astron. Astrophys.* **269**(1993)67;
 Kirk, J.G. and Lyubarsky, Y.: *Publ. Astron. Soc. Austr.* **18**(2001)415;
 Lyubarsky, Y.: *Mon. Not. Roy. Astron. Soc.* **345**(2003) 153;
 Dermer, C. and Schlickeiser, R. *Astrophys. J.* **416**(1993)458;
 Blandford, R.D. and Levinson, A.: *Astrophys. J.* **441** (1995)79;
 van Putten, M.H.P.M.: *Phys. Rep.* **345**(2001)1;
 van Putten, M.H.P.M.: *Phys. Rev. Lett.* **84**(2000)3752;
 Punsly, B. and Coroniti, F.V.: *Astrophys. J.* **350**(1990)518.
- [18] Blandford, R.D.: *ASP Conf. Ser. 160, Astrophysical Disks*, eds. Sellwood, J.A. and Goodman, J. (San Francisco: ASP, 1999)265;
 Gruzinov, A.: (astro-ph/9908101);
 Li, L.-X.: *Astrophys. J.* **533**(2000)L115;
 Li, L.-X.: *Astrophys. J.* **540**(2000)L17.
- [19] Zhang, X.-H.: *Phys. Rev.* **D39**(1989)2933.
- [20] Zhang, X.-H.: *Phys. Rev.* **D40**(1989)3858.
- [21] Lee, H.K., Wijers, R.A.M.J., and Brown, G.E.: *Phys. Rep.* **325**(2000)83.
- [22] Lee, H.K., Brown, G.E., Wijers, R.A.M.J.: *Astrophys. J.* **536**(2000)416.
- [23] Lee, H.K., Wijers, R.A.M.J. and Brown, G.E.: *ASP Conf. Series, 190, Gamma-Ray Bursts: The First Three Minutes* eds. Poutanen, J. and Svensson, R. (San Francisco: ASP, 1999)173.

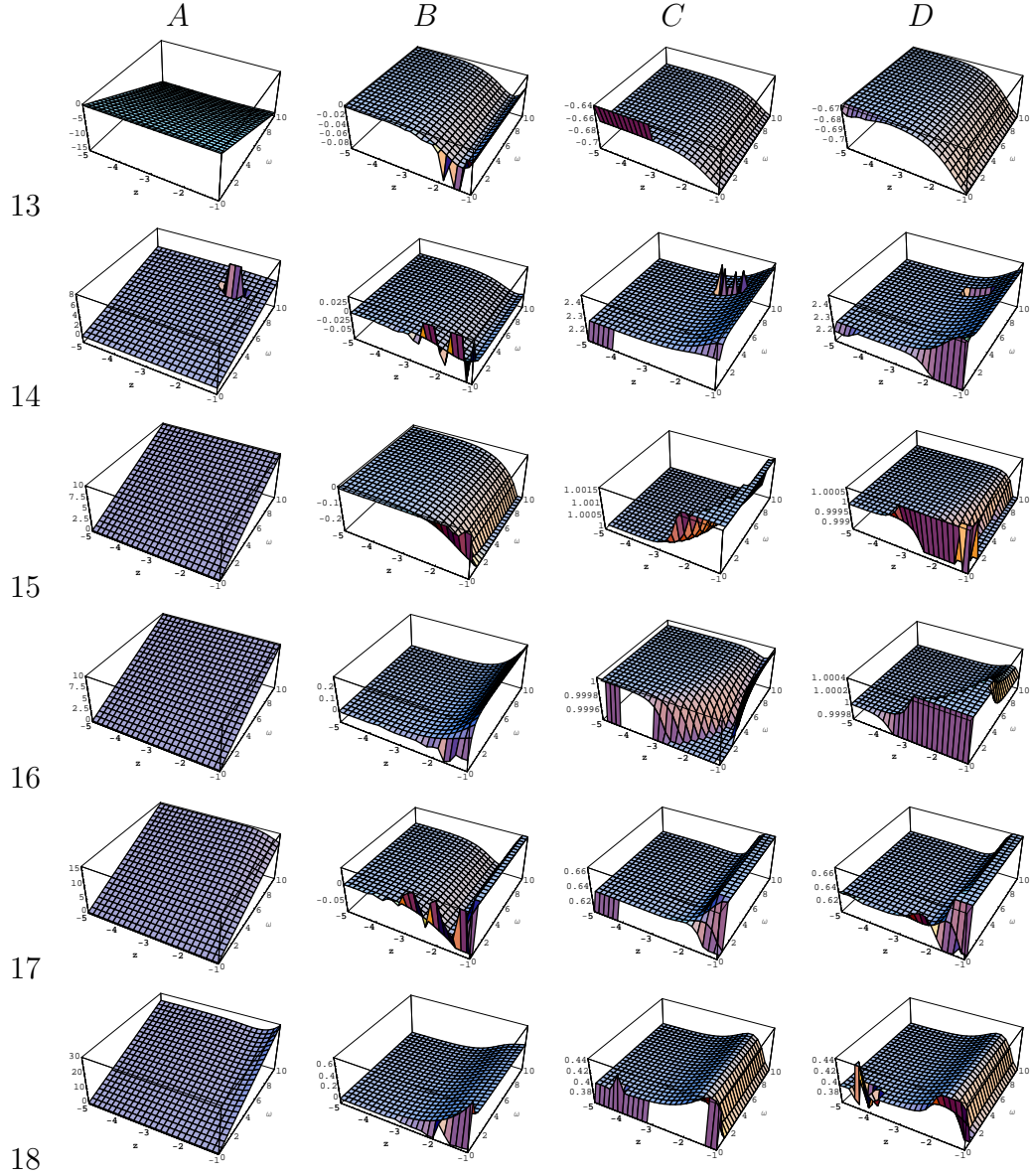
- [24] Wilms, J., Reynolds, C.S., Begelman, M.C., Reeves, J., Molendi, S., Staubert, R. and Kendziorra, E.: Mon. Not. R. Astron. Soc. 328(2001)L27.
- [25] Perlman, E. S., Sparks, W. B., Radomski, J., Packham, C., Fisher, R. S., Piña, R. and Biretta, J.A.: Astrophys. J. 561(2001)L51.
- [26] Junor, W., Biretta, J. A. and Livio, M.: Nature 401(1999)891.
- [27] Koide, S., Shibata, K., Kudoh, T. and Meier, D.L.: Science **295**(2002)1688.
- [28] Sharif, M. and Sheikh, U.: Gen. Relat. Gravit. **39**(2007)1437; *ibid* 2095; Int. J. Mod. Phys. **A23**(2008)1417; J. Korean Phys. Soc. **52**(2008)152; *ibid* **53**(2008)2198; Sharif, M. and Mustafa, G.: Canadian J. Phys. **86**(2008)1265.
- [29] Sheikh, U.: Ph.D. thesis. University of the Punjab, Lahore, Pakistan (2008).
- [30] Sharif, M. and Sheikh, U.: *Cold Plasma Gravitomagnetic Waves in Kerr Planar Analogue*, submitted for publication.
- [31] Sharif, M. and Sheikh, U.: *Cold Plasma Wave Analysis in Magneto-Rotational Fluids*, submitted for publication.
- [32] Sharif, M. and Sheikh, U.: Class. Quantum Grav. **24**(2007)5495.
- [33] Das, A.C.: *Space Plasma Physics: An Introduction* (Narosa Publishing House, New Delhi, 2004).
- [34] Veselago, V.G.: Sov. Phys. Usp. **10**(1968)509.
- [35] Achenbach, J.D.: *Wave Propagation in Elastic Solids* (North-Holland Publishing Company, Oxford, 1973).
- [36] Shelby, R.A., Smith, D.R. and Schultz, S.: Science **292**(2001)77.



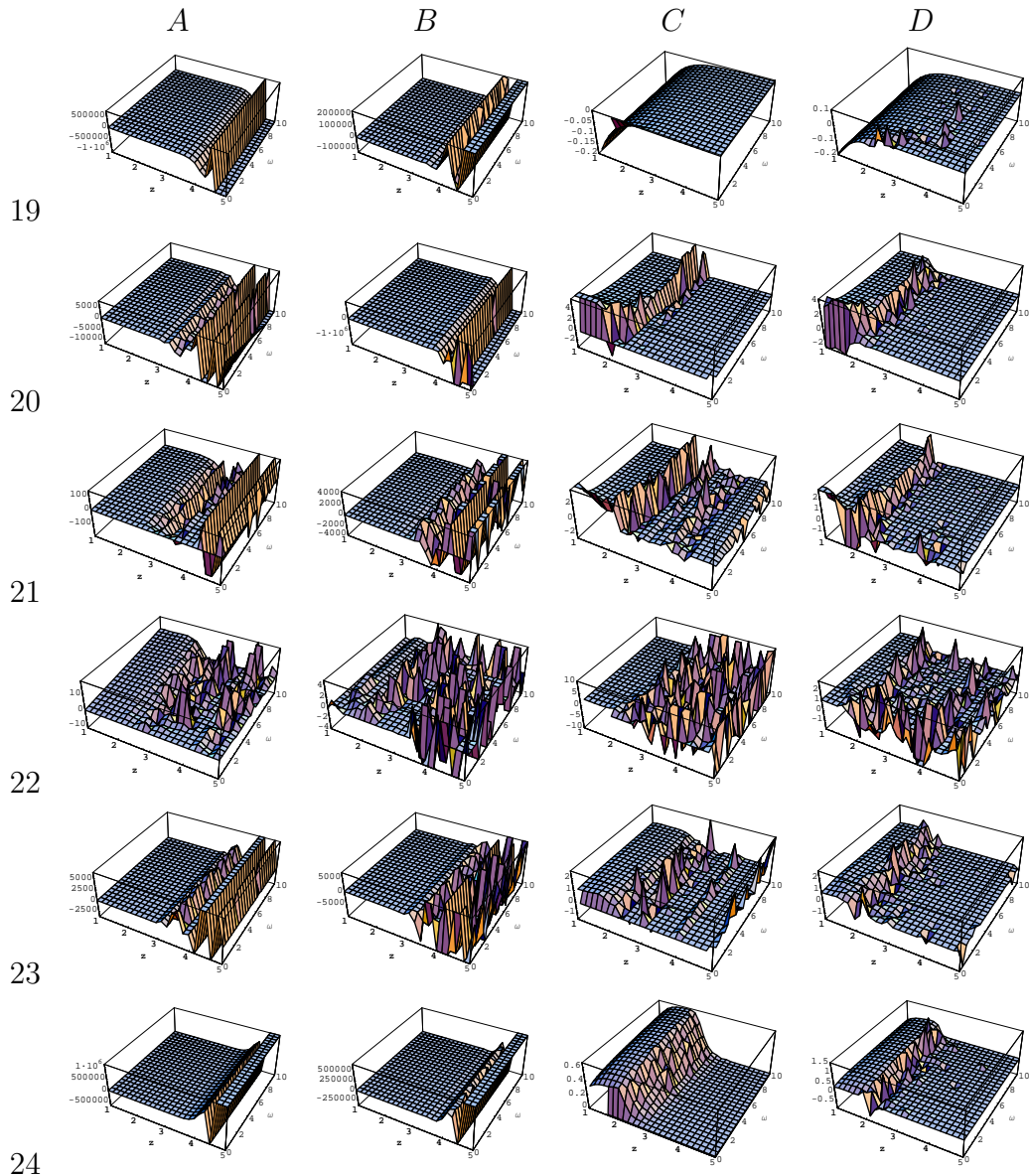
Figures 1-6 show the dispersion relations (related to the velocity components given by Eq.(3.3)) in the neighborhood of the pair production region towards the event horizon.



Figures 7-12 indicate the dispersion relations (related to the velocity components given by Eq.(3.3)) in the neighborhood of the pair production region towards the outer end of the magnetosphere.



Figures 13-18 represent the dispersion relations (related to the velocity components given by Eq.(3.4)) in the neighborhood of the pair production region towards the event horizon.



Figures 19-24 show the dispersion relations (related to the velocity components given by Eq.(3.4)) in the neighborhood of the pair production region towards the outer end of the magnetosphere.